

Irena Nikcevic¹
Aigars Piruska¹
Kenneth R. Wehmeyer²
Carl J. Seliskar¹
Patrick A. Limbach¹
William R. Heineman¹

¹Department of Chemistry,
University of Cincinnati,
Cincinnati, OH, USA

²Mason Business Center, Procter
and Gamble Pharmaceuticals,
Mason, OH, USA

Received January 20, 2010

Revised May 25, 2010

Accepted May 26, 2010

Research Article

Parallel separations using capillary electrophoresis on a multilane microchip with multiplexed laser-induced fluorescence detection

Parallel separations using CE on a multilane microchip with multiplexed LIF detection is demonstrated. The detection system was developed to simultaneously record data on all channels using an expanded laser beam for excitation, a camera lens to capture emission, and a CCD camera for detection. The detection system enables monitoring of each channel continuously and distinguishing individual lanes without significant crosstalk between adjacent lanes. Multiple analytes can be determined in parallel lanes within a single microchip in a single run, leading to increased sample throughput. The pK_a determination of small molecule analytes is demonstrated with the multilane microchip.

Keywords:

CE / Fluorescence detection / Multilane microchip / pK_a determinations

DOI 10.1002/elps.201000030



1 Introduction

Miniaturization of analytical devices is a trend that emerged in the beginning of the 1980s [1, 2]. The advantages of these devices include improved performance, reduced sample amount, shorter analysis time, and reduced cost.

CE is a separation method that discriminates chemical entities based on their electrophoretic mobility under an applied electric field. CE is better suited for miniaturization (flow rate proportional to d^2) than pressure-driven separation methods (d^4), where d is the inner diameter of the column/channel. CE has been used in numerous chemical and biological applications, such as separation of proteins and peptides [3, 4], chiral analysis of optical impurities [5], peptide mapping of biopharmaceutical drugs [6, 7], DNA analysis [8], and organic acid analysis [9].

The migration of CE to a microchip platform has gained increasing attention during the past decade [10–15]. It can provide more rapid analysis than traditional CE, requires minimal sample amounts, and can be automated similarly to traditional CE. Additionally, MCE can integrate a variety

of laboratory procedures and pretreatment steps on a single microchip, and it offers the promise of transferring this technology to a cheap, disposable plastic substrate [10–15].

Despite its short analysis time, MCE, like CE, is intrinsically a sequential technique (each of the networks can perform the analysis of only one sample at a time, *i.e.* sequentially), and the majority of analyses have been demonstrated on a single-lane chip capable of performing only one analysis or separation at a time. However, parallel separations are desirable for real-world applications, such as high-throughput genetic and proteomic analyses, food analyses, peptide mapping, screening of drug candidates, *etc.* Parallel separations on a multilane microchip are a promising alternative for enhancing sample throughput. Advances in microfabrication techniques [10, 16, 17] enable fabrication of a large number of channels on a single chip with little added cost, while significantly increasing sample-throughput due to parallelization of an assay. Several groups have developed multilane chips for immunoassays [18] and genomic analysis [14, 19, 20] that demonstrate the advantages of MCE. In contrast to traditional CE where UV absorption detection is the most commonly used detection method, MCE almost exclusively uses fluorescence spectroscopy (especially LIF) for detection. Typically in microchip CE, LIF is used for detection as UV detection is not sensitive enough due to the short optical path length. Various methods for multilane detection have been reviewed recently [21]. There are two major ways to achieve multilane LIF detection with microfluidic devices: (i) using a single

Correspondence: Professor William R. Heineman, Department of Chemistry, University of Cincinnati, P.O. Box 210172, Cincinnati, OH, USA

E-mail: William.Heineman@uc.edu

Fax: +1-513-556-9239

Abbreviation: OG, Oregon green

lane detection system and scanning each lane separately or (ii) exciting multiple lanes and detecting fluorescence with an imaging detector. In the case of the single lane configuration, the system can be modified to accommodate detection for multilane chips. In essence, all these modifications include movement of the focused excitation beam with respect to the microchip. The chip itself can be translated to avoid changes in the optical setup [20] or the excitation beam position can be scanned with a galvoscaner [14, 22], an acousto-optical device [23], or rotated around the chip [24, 25]. The mechanical translation movement of a chip or a detector is limited to low scanning rates. In addition, mechanical noise (*e.g.* jitter and wobble) can distort the signal. An elegant solution for a moving detector was demonstrated by Mathies *et al.* [24, 25]. A microscope objective was rotated around a multilane microchip with radial symmetry. The excitation was delivered along the rotation axis and deflected to the objective by a rhomb prism. High scan rates, position accuracy, and speed uniformity were achieved. An acousto-optical device [23] deflects the excitation beam according to an applied frequency, which provides fast switching (on the order of nanoseconds) from one channel to another, self calibration, and random channel scanning. These benefits come with the cost of uneven illumination intensity across channels that, in turn, requires normalization of the raw signal.

LIF with an imaging detector has proven to be useful in a variety of capillary and slab gel electrophoresis applications, and recently, on microchips. Several commercial instruments are available for CE dedicated to gene sequencing [26]. CCD cameras have been used to detect fluorescence from several capillaries [27] or to monitor capillary isoelectric focusing on an entire column [28] with a detection limit of 10^{-11} M. Ewing *et al.* demonstrated that DNA separation can be detected with a CCD camera on an ultra thin gel slab by expanding the laser beam and focusing the light strip on the gel slab [29] or large chip [30]. The advantage of this scheme is that separation is detected in parallel without implementing moving parts, and the configuration of channels on the chip does not affect detection. Recently, Dang *et al.* demonstrated genetic analysis on a multilane plastic microchip with an imaging detector [31, 32]. The detection was achieved by focusing a linearly expanded laser beam on an array of parallel channels.

This paper demonstrates a LIF detection system for parallel separation on a multilane MCE. Optical detection was achieved by exciting all channels simultaneously with an expanded laser beam. The emission signal was captured with a camera lens and detected with a CCD camera. This detection setup enables monitoring each channel continuously and distinguishing the signals from individual lanes without significant crosstalk between adjacent lanes. Multiple analytes can be determined in parallel lanes within a single microchip in a single run, leading to increased sample throughput. The pK_a determination of small molecule analytes is demonstrated using this detection system.

2 Materials and methods

2.1 Reagents and solutions

OG (Oregon green 488, dextran conjugate, MW = 10 000, D-7170), 5-(and-6)-carboxy SNARF-1 (C-1270) and BP (Bodipy 505/515, D-3921) were obtained from Invitrogen (Carlsbad, CA, USA). Fluorescein (FL) was from Sigma-Aldrich (Milwaukee, WI, USA). Sodium hydroxide, analytical grade, was from Fisher (Pittsburgh, PA, USA), methanol, HPLC-UV grade, was from Pharmco (Brookfield, CT, USA), and ethanol was from Aaper alcohol (Shelbyville, KY, USA). A wide screen pK_a buffer kit was obtained from Combisep (Ames, IA, USA). The kit consisted of 12 individual buffers from pH 2.10 to 10.80 adjusted to a constant ionic strength of 50 mM. The running buffer was prepared by $5 \times$ dilutions of purchased solutions. Deionized water was obtained using a Barnstead water purification system (18 M Ω) (Sybron/Barnstead, Boston, MA, USA). All solutions used in experiments with microchips were filtered through a 0.45- μ m syringe filter (Millipore, Bedford, MA, USA). The running buffer and water were degassed offline prior to experiments by adding 4–6 mL of either running buffer or water to a 10 mL syringe, plugging the syringe hole, pulling the plunger back to create a vacuum, and then tapping the syringe with a pen or an empty syringe. The process was repeated until the solution was free of air bubbles. Stock solutions were freshly prepared before use. The desired concentration of dyes was achieved by dissolving the filtered stock solution with filtered water or running buffer. Diluted samples were not filtered due to the strong adsorption of dye on the syringe filter. BP was dissolved in ethanol to make a stock solution. FL, OG, and SNARF-1 were dissolved in deionized water. Appropriate aliquots of each stock solution were mixed and diluted with water and 10% running buffer to give a sample solution. Prior to experiments, a multilane chip was conditioned with filtered 1 M sodium hydroxide (10 min), deionized water (10 min), and running buffer (10 min). Liquids were moved through the chip by applying suction on the common reservoir using a vacuum pump (DAA model, Gast, Benton Harbor, MI, USA). Between conditioning steps, reservoirs of the chip were rinsed with the solution used for the subsequent conditioning step. After experiments were completed, channels were flushed with methanol (10 min) and deionized water (10 min). Chips were stored dry.

2.2 Multilane detection setup

The schematic of the multilane detection setup is shown in Fig. 1. A beam from a 488-nm Ar-ion laser (Melles Griot, Carlsbad, CA, USA) was passed through three lenses (Powell lens with fan angle of 5° (Lasiris, St-Laurent, QC, Canada); concave cylinder lens (focal length=25 mm; Edmund Optics, Barrington, NJ, USA); convex cylinder lens (focal length 25 mm; Edmund Optics)) to form the beam into a linear shape with approximately uniform intensity across the long axis. The cylinder lenses were oriented to focus the fan

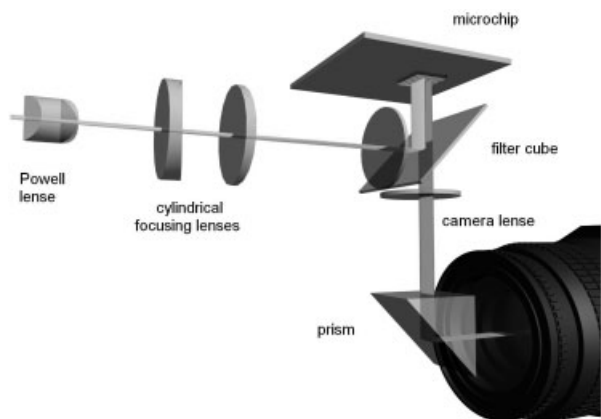


Figure 1. Scheme of the multilane detection setup.

generated by the Powell lens into a linear shape (the fan is generated perpendicular to the paper plane, see Fig. 1). The reshaped beam and emission were filtered with a laser filter set at 488 nm (excitation filter z488/10 ×; dichroic mirror z488rdc; emission filter hq525/50 m; Chroma, Rockingham, VT, USA). Emission generated was reflected with a prism (BK7; 45–90–45°; entrance and exit face 1" × 1"; Edmund Optics.) and collected with a 60 mm AF Micro Nikkor camera lens (Nikon, Melville, NY, USA) and imaged onto a CoolSnapHQ CCD (Roper Scientific, Trenton, NJ, USA). Laser power was measured at the sample with a PM-300 power meter (Kimmon Electric Co., Centennial, CO, USA). High voltage was applied with an HVS448 3000 power supply (LabSmith, Livermore, CA, USA). The separation sequence was programmed in Sequence (LabSmith) and initiated from a data acquisition program written in LabView (National Instruments, Austin, TX, USA). Data was acquired by a home written software by a Scientific Imaging Tool Kit (R Cubed Software Consultants, Lawrenceville, NJ, USA) and LabView (National Instruments).

2.3 Multilane chip

Dyes were separated on custom designed and fabricated glass multilane chips purchased from The Dolomite Centre (Royston, Herts, UK). The details of the multilane chip design are illustrated in Fig. 2. The multilane chip consisted of eight lanes of equal lengths with a channel width and depth being 60 and 20 μm, respectively. The reservoir holes are 2.5 mm in diameter, and the common reservoir is 5 mm in diameter. To simplify fluid handling and suppress Laplace pressure effects on the separation [15], an 11 mm-thick cover plate was bonded to the glass microchip resulting in 54 μL reservoirs. Voltages were applied to the microfluidic channels through platinum electrodes using a HVS 488–3000 power supply (LabSmith, Livermore, CA, USA). A custom ordered circuit board PCB123, Mulino, OR, USA) was used to specify each electrode position and all

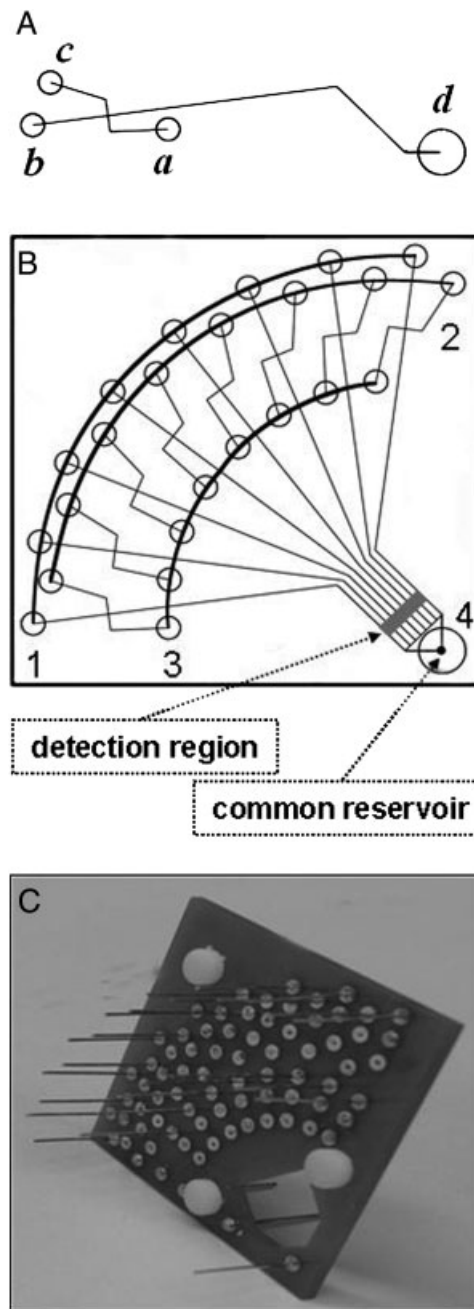


Figure 2. Schematic of the multilane chip design. (A) Layout of a single lane with the reservoir abbreviations: sample (a), buffer (b), sample waste (c), and buffer waste, common reservoir (d). The distances from the reservoirs to the center of the intersection are 8 mm for a, b, and c and 38 mm from reservoir d (separation channel). The diameters of the reservoir holes are 2.5 mm and of the common reservoir, 5 mm. The channel width and depth are 60 and 20 μm, respectively. (B) Multilane chip layout with scheme of electrode setup to apply separation voltage program. Each set of electrodes is subject to a specific potential (1 – buffer, 2 – sample waste, 3 – sample, and 4 – buffer waste). (C) picture of electrode circuit board.

electrodes were divided in four independent sets (Fig. 2C) so only four voltage channels are needed to drive separations.

A 14-lane chip prepared in-house (Y. Abdelaziez *et al.*, unpublished data) (60×80 mm glass chip with $20 \mu\text{m}$ channel height, $60 \mu\text{m}$ channel width, 1.1 mm thick glass cover plate, and reservoir diameter of 1.5 mm, see Supporting Information) and a circuit board similar to the one described for the 8-lane chip were also used in these studies. The 14-lane chip was used primarily for characterization of the multilane detection system because the lanes in the detection region are closer (14 lanes in 6 mm) than in the 8-lane chip design (8 lanes in 5.6 mm). The plastic plate (~ 11 mm thick) with appropriate hole pattern was glued on the chip and served as add-on reservoirs for the chip. The details of this multilane chip design are found in the Supporting Information.

2.4 Multilane detection setup characterization

Field of view and *resolution* were characterized by placing an inverse resolution target (Edmund Optics) or a photocopy of a ruler on the sample stage and acquiring the image. The *beam profile* was determined by placing a 5.0-mm-thick polycarbonate piece on the sample stage and recording the plastic autofluorescence. The *crosstalk* between lanes was evaluated by filling channels with 2×10^{-8} and 1×10^{-7} M fluorescein solution in a glass multilane chip and acquiring the sequence of channel images under 488 nm excitation. Fluorescein solutions with concentrations from 50 nM to $10 \mu\text{M}$ were used in this experiment. The *dynamic range* of the system was demonstrated by flowing various concentrations of fluorescein solution through the microchip and detecting the fluorescence response.

2.5 Demonstration of multilane chip separation feasibility for estimations of pK_a

OG 488 (dextran conjugate), 5 (and 6)-carboxy SNARF-1 and fluorescein were used as model compounds to estimate the pK_a . Bodipy 505/515 was used as a neutral marker and was chosen to match the laser used. A wide screen pK_a buffer kit (pH 2.10–10.80) was diluted to 10 mM to prepare the running buffer. An ionic strength of 10 mM was a compromise between sufficient buffer capacity and low Joule heating. The pH was measured with an Accumet XL 50 pH meter (Fisher, Pittsburgh, PA, USA). The dyes were diluted to $15 \mu\text{M}$ (neutral marker) and $30 \mu\text{M}$ (analyte) in deionized water and 10% of the appropriate buffer solution with different pHs. The pK_a values were estimated using non-linear and linear regression.

3 Results and discussion

3.1 Multilane chip designs

For the convenience of simultaneous excitation and detection of analytes on all channels with a single expanded laser

beam, several multilane chip designs with closely spaced channels in the detection region were considered. The distance between the outer edges of the first and the last channels in the detection region was 5.6 mm in all designs. Initially, the multilane pattern was designed to fit vertically on 50×50 mm chips (see Supporting Information). To simplify fluid handling and to reduce the possibility of solution cross-contamination and accidental short circuiting, the distance between reservoirs was maximized. One option was to move a set of buffer reservoirs down by 2.5 mm, or to move down both sets of sample waste and buffer reservoirs by 2.5 mm (see Supporting Information). However, the diagonal pattern concept with increased angle between channels was chosen (Fig. 2A). To reduce the problem of a possible siphoning effect, a common outlet reservoir was designed to be twice as large as the inlet reservoirs.

The 14-lane chip design (see Supporting Information) (Y. Abdelaziez *et al.*, unpublished data), where each lane had separate reservoirs, was also considered for pK_a studies, but was eventually discarded for the pK_a studies because it required attaching additional numerous reservoirs in close proximity leading to more liquid handling problems, and Laplace pressure effects.

3.2 Characterization of multilane detection system

The multilane detection setup was designed for simultaneous excitation and detection of fluorophores in several microfluidic channels. The emission from individual lanes was monitored with an imaging detector, thus avoiding the need for moving parts in the excitation or detection setups and allowing simultaneous and continuous detection of all lanes.

Beam expansion was achieved with a three-lens system. Initially, the beam was expanded orthogonally to its propagation direction using a Powell lens, creating a diverging fan

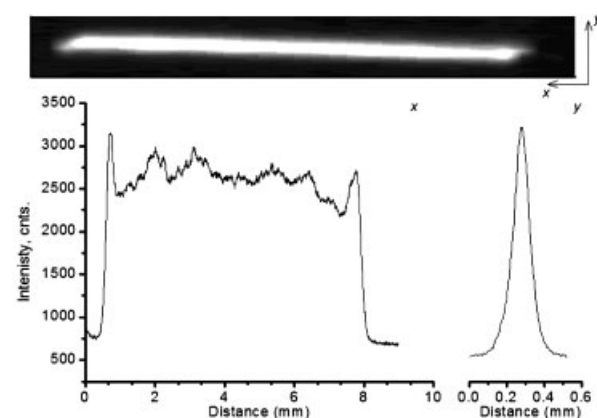


Figure 3. Characteristics of the excitation beam. Top image shows grayscale image of the laser beam – fluorescence from polycarbonate sheet. Two bottom panels are cross section of the beam parallel to long (x) and short (y) axes.

with an angle of 5° . This fan was expanded with a convex cylinder lens and then refocused with a concave cylinder lens. The focusing and expansion by cylinder lenses was done in an orthogonal direction with respect to both beam propagation and initial expansion. As a result of these beam manipulations, a narrow excitation line was formed. The beam profile is shown in Fig. 3.

The main advantage of using a Powell lens instead of a cylinder lens is that a fairly uniform excitation beam profile along the long axis of the excitation beam is achieved [33, 34]. The conical lens diverges more intensity from the center of the beam to the sides, thus large distances could be illuminated at comparable intensity without wasting laser power. Spatial variation of beam intensity is significant (up to 20%); however, the pK_a determination requires information about migration time only, not quantity or concentration. For applications where concentration information is important, the use of an internal standard would be required to normalize the spatial variation in beam intensity. The full width of the beam is approximately $150\ \mu\text{m}$ (Fig. 3). This value could be an overestimation of the actual width of the peak due to measurement of the profile in the plastic sheet.

The emission was collected with a close-up camera lens, allowing close to 1:1 imaging of separation channels on the CCD chip. An area approximately $9\ \text{mm} \times 6\ \text{mm}$ could be monitored through the camera lens, which was sufficient for observation of all eight lanes simultaneously (see Supporting Information). The resolution of this setup was 8 lines/mm, measured with a negative 1951 USAF target (Edmund Optics) (for comparison, the resolution of Nikon TE-2000 epifluorescence microscope with $10\times$ objective is 64 lines/mm).

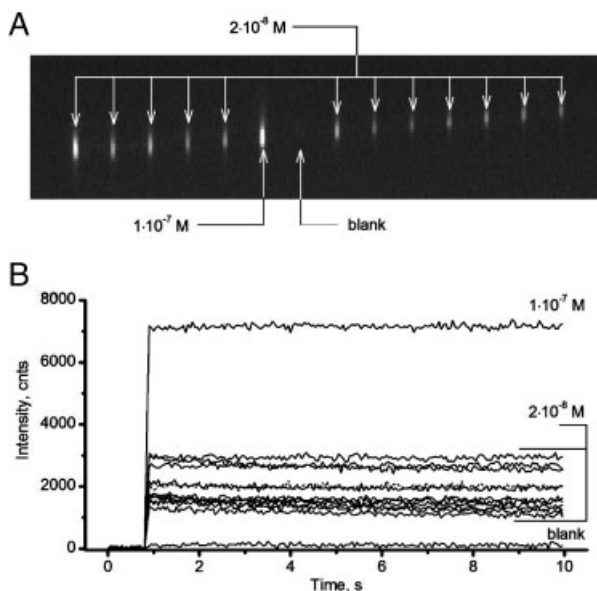


Figure 4. Evaluation of crosstalk between adjacent lanes: (A) image of channels filled with fluorescein; (B) signal from individual lanes over time.

The simultaneous excitation of fluorophores in close vicinity can lead to crosstalk between adjacent channels. To evaluate the significance of this issue, fluorescein was flowed through all channels of the 14-lane microchip as shown in Fig. 4. In Fig. 4A, the signal from each channel is clearly separated from all other channels and no significant crosstalk is observed. The lack of detection crosstalk is most clearly shown in the blank channel, which is next to a high concentration channel. These results are consistent with the previously determined resolution of the setup using a negative target. Even when fluorophore concentration was increased up to few tens μM , no significant crosstalk was observed. Signal intensity in each channel *versus* time is reported in Fig. 4B. The variation in intensity among the channels containing the $2 \times 10^{-8}\ \text{M}$ fluorescein is due to the spatial variation of the beam intensity across the lanes. It is worth mentioning that the beam profile shown in Fig. 3 exhibits less variation ($\sim 35\%$) than the fluorescence signal from different microchannels ($\sim 100\%$). However, the beam profile was obtained by illuminating a thick piece of fluorescing material. The large field depth of the camera lens ensures that the measurement is relatively insensitive to the orientation of the excitation beam focal volume. However, in the case of the multilane microchip, deviations of the focal volume off the plane formed by a parallel region of the microchannels would contribute to an additional variation in the excitation intensity.

The dynamic response of the system was evaluated by flowing fluorescein at various concentrations through the 14-lane microchip. The results are summarized in Fig. 5. The limit of detection is 30 nM and the dynamic range is 2 orders of magnitude. The detection can be performed in a concentration range from high nanomolar to micromolar, and it is primarily limited by the collection efficiency of the camera lens and low irradiance. Single lane detection provides more flexibility to optimize the measurement, *e.g.* spatial filtering, larger range of illumination power density, and better collection efficiency. Some of this flexibility is sacrificed in the multilane setup in order to obtain simultaneous detection over a large spatial area. The loss of linearity at the lower nanomolar concentrations is likely due to adsorption of the fluorescein on the reservoirs and channels.

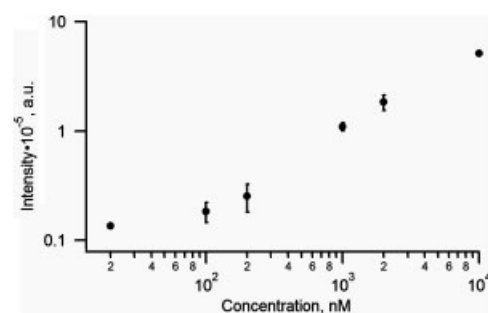


Figure 5. Fluorescence intensity at various concentrations of fluorescein in multilane chip.

3.3 Electrophoretic separation

All electrophoretic experiments on the glass multilane chip were carried out under the same separation conditions. A pinched injection scheme was used for all electrophoretic separations. Fifty-micromolar fluorescein was used to optimize the voltage configuration. Voltages for injection were determined by observing the appearance of the sample plug in the channel intersection when the sample solution was driven from the sample reservoir to the sample waste reservoir. The well-defined sample plug at the cross section partially fills the boundaries of the upper and lower portions of the separation channel. The injection voltage scheme was optimized by adjusting voltages until the desired plug shape was achieved and there was no sample leaking into the separation channel. The separation voltage scheme was determined by adjusting voltages so that the sample entrapped in the cross section was pushed into the separation channel.

The optimized voltage configuration for each lane (Fig. 2b) is shown in Table 1. Voltages were applied to the microfluidic channels through four sets of electrodes connected to the appropriate reservoirs (Fig. 2C). Injection was initiated by applying 1.5 kV to the sample reservoir (a), 1.2 kV to the buffer reservoir (b), 1.7 kV to the buffer waste reservoir (d), and grounding the sample waste reservoir (c) for 35 s until the sample solution flow reached a steady state. During the separation process, 1.5 kV were applied to the a and c reservoirs, and 3 kV were applied to the b reservoir, while grounding the d reservoir.

3.4 Rapid pK_a determination using CE multilane chip

The determination of pK_a values by CE relies on the principle that acid and base forms of a candidate compound have different electrophoretic mobilities. The pK_a values can be obtained by fitting the plot of effective mobility *versus* pH to a suitable model for the number of ionizable groups [35–39].

The separation of the analyte and neutral marker in a series of buffers that have a constant ionic strength but different pHs was used to demonstrate the feasibility of pK_a determinations in the 8-lane multilane chip. Measuring the migration times of the analyte and the neutral marker, for a series of buffers at different pHs, can provide the effective

Table 1. Conditions for electrophoretic separations on the multilane chip

	Injection	Separation
V_A (kV)	1.5	1.5
V_B (kV)	1.2	3
V_C (kV)	grnd	1.5
V_D (kV)	1.7	grnd
Time (s)	35	55

electrophoretic mobility of an ionic form, μ_e . The pK_a is determined from sigmoidal fitting of μ_e *versus* pH using a non-linear regression for

$$\mu_e = \frac{\mu_a}{10^{(pK_a - pH)} + 1} \quad (1)$$

where μ_a is the electrophoretic mobility of the fully deprotonated species A^- . μ_a and pK_a are obtained as the regression parameters. pK_a values can also be calculated using the linear regression method for the equation

$$\frac{1}{\mu_e} = \frac{1}{K_a \mu_a} [H^+] + \frac{1}{\mu_a} \quad (2)$$

Therefore, the pK_a value can be obtained by plotting $1/\mu_e$ *versus* $[H^+]$, where $K_a \mu_a$ is the slope and $1/\mu_a$ the intercept.

Equations (1) and (2) are valid for pH values where only the neutral and the monovalent forms coexist and the concentrations of other species are negligible in this pH range. In the case of a polyprotic compound $H_n X^z$, coexisting in different ionized states at given pH, the effective mobility is

$$\mu_e = \sum_{i=0}^n \frac{\left[\prod_{j=1}^i 10^{-pK_{aj}} \right] \times 10^{(i-n)pH}}{\sum_{i=0}^n \left[\prod_{j=1}^i 10^{-pK_{aj}} \right] \times 10^{(i-n)pH}} \times \mu_{H_{(n-i)} X^{z-i}} \quad (3)$$

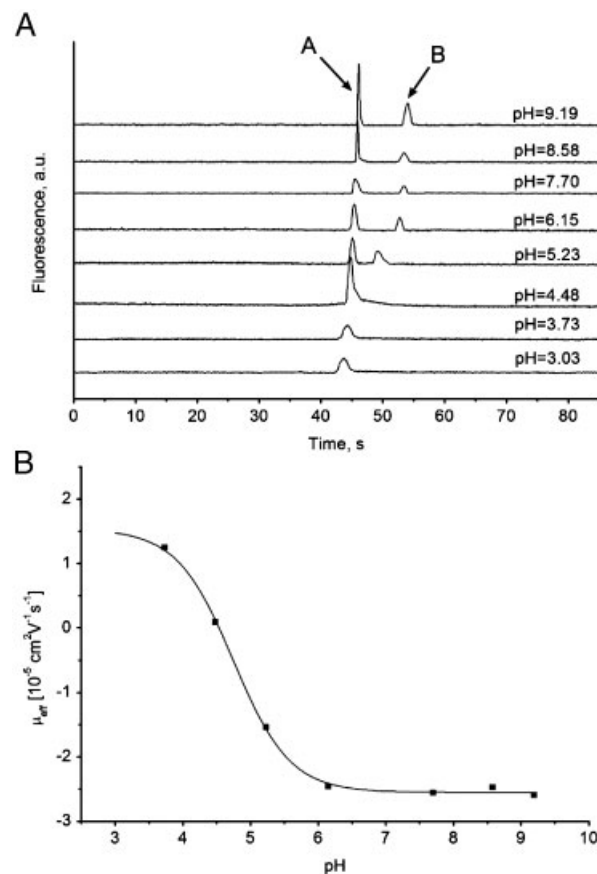


Figure 6. (A) The separation of OG 488 (dextran conjugate, 10 000) and BP on a multilane chip with LIF detection. The electropherograms are offset to illustrate the separation for each lane. A is BP and B is OG. (B) Plot of effective mobility *versus* pH to obtain pK_a value by CE multilane microchip with LIF detection.

where n is the total number of ionizable groups and z the charge of the fully protonated species [40, 41]. This equation allows the determination of pK_a values from a plot of μ_e as a function of pH. It can be applied to different ionizable compounds as shown in the Supporting Information.

Figure 6A shows the result of OG (30 μ M) and BP (15 μ M) MCE separation. All separations were done in a single run on the glass multilane microchip with an effective channel length of 2.8 cm at a field strength of 566 V/cm. Each microchip lane was filled with a different pH buffer. The first 35 s represents the injection after which the separation step starts. As the pH drops, peak B (OG) intensity decreases slightly while shifting toward peak A (BP). Peaks A and B merged at pH \sim 4.5 and they coeluted below pH4. A slight variation in signal intensity, which comes from a varying magnitude of baseline noise, was also observed.

The pK_a values of the analyte were determined by comparing the migration times of the analyte and the neutral marker over a specific range of pH in a single run. A neutral marker of the EOF was used to calculate the electrophoretic mobility of the analyte as a function of pH. The migration time of the neutral BP peak changes with EOF. The migration of the analyte OG peak relative to the BP peak varies with pH. The intensity of OG peaks decreases as the pH is lowered. The effective mobility of OG was determined and plotted versus pH (Fig. 6B). A non-linear regression analysis was used to calculate the pK_a value. The calculated value was determined as 4.72, which agrees well with a literature pK_a value of 4.7 (www.invitrogen.com).

The feasibility of determining pK_a values by multilane glass chip with LIF detection was demonstrated for two other compounds. A non-linear regression was used for pK_a determination of SNARF-1, while linear regression analysis was used in the case of FL, since its quantum yield is significantly reduced at pHs below its pK_a . A linear regression model can result in discrepancies between the data obtained and literature values [38]. However, these discrepancies can be eliminated if data are collected in a narrow pH range [42]. The data for FL were collected in a pH range from 6.0 to 9.2. Table 2 summarizes the pK_a values obtained using the multilane microchip. These values are in good agreement with literature values (www.invitrogen.com) [43, 44].

In comparison with the pK_a determination on a single lane chip where the total time to complete one compound

was 3–4 h [37] because each buffer had to be used separately with conditioning, the throughput provided by the multilane microchip was significantly increased. The pK_a value for one compound was determined in a few minutes. The 8-lane chip with a diagonal pattern design and a common outlet reservoir appeared to be a good choice for successful determination of pK_a values. In the present configuration, the multilane CE microchip method offers increased daily throughput over a single-lane CE method. It is expected that sample throughput will increase further by automating the liquid delivery and increasing the number of lanes in the chip. For broad applicability to a wide range of small molecular weight compounds that includes those that do not fluoresce, it will be necessary to implement a UV detection system in place of the LIF detection system. For pK_a determinations this should not be a problem as high concentrations of compound can be used for these experiments.

4 Concluding remarks

A multilane detection system for the determination of pK_a using LIF detection on multilane microchips was developed as a model system for the evaluation of rapid pK_a determination via MCE. The 8-lane microchip LIF design is just a prototype. The ultimate goal is to implement UV detection for broad applicability to small molecules that do not exhibit fluorescence. Typically, UV detection lacks sensitivity in MCE, however, for pK_a determinations relatively high concentrations can be employed and, therefore, detection limit is less of an issue. Additionally, increases in speed and throughput can be obtained by using disposable plastic chips instead of glass to eliminate the need for chip cleaning (reservoir and channel washing) and the use of automated liquid handling to allow continuous operation.

Financial support of this research was provided by the National Institutes of Health (Grant GM 69547). Thanks to Paul McKenzie from the electronics shop and Bill Brauntz from the machine shop (Department of Chemistry, University of Cincinnati) for help with electrode circuit board design and construction. The authors also thank Phil Homewood and Mark Gilligan from The Dolomite Centre Ltd for help with aspects of chip design.

The authors have declared no conflict of interest.

Table 2. pK_a values determined by multilane CE microchip^{a)}

Compound	Literature pK_a	Multilane chip pK_a
Oregon green 488	4.7 ^{b)}	4.72 \pm 0.03
5-(and-6)-carboxy SNARF-1	7.5 ^{b)}	7.53 \pm 0.05
Fluorescein sodium salt	6.4–6.6 [44, 45]	6.5 \pm 0.11

a) $n = 3$ replicate determinations of pK_a for each compound.

b) www.invitrogen.com

5 References

- [1] Nguyen, N.-T., Wereley, S. T., *Fundamentals and Applications of Microfluidics*, Artech House, Boston, MA 2002.
- [2] Abgrall, P., Gué, A.-M., *J. Micromech. Microeng.* 2007, 17, R15–R49.

- [3] Ostergaard, J., Jensen, H., *Anal. Chem.* 2009, *81*, 8644–8648.
- [4] Mosca, A., Paleari, R., Mosca, L., Marcello, A., Vercellati, C., Zanella, A., *Clin. Biochem.* 2009, *42*, 1859.
- [5] Zha, Y., Yang, X. B., Jiang, R., Sun, X. L., Li, X. Y., Liu, W. M., Zhang, S. Y., *Chirality* 2006, *18*, 84–90.
- [6] Deyl, Z., Tagliaro, F., Miksik, I., *J. Chromatogr. B* 1994, *656*, 3–27.
- [7] Migneault, I., Dartiguenave, C., Vinh, J., Bertrand, M. J., Waldron, K. C., *J. Liq. Chromatogr. Relat. Technol.* 2008, *31*, 789–806.
- [8] Fattorini, P., Marrubini, G., Ricci, U., Gerin, F., Grignani, P., Cigliero, S. S., Xamin, A., Edalucci, E., La Marca, G., Previdere, C., *Electrophoresis* 2009, *30*, 3986–3995.
- [9] Buchinger, S., Follrich, B., Lammerhofer, M., Lubda, D., Lindner, W., *Electrophoresis* 2009, *30*, 3804–3813.
- [10] Jacobson, S. C., Culbertson, C. T., Daler, J. E., Ramsey, J. M., *Anal. Chem.* 1998, *70*, 3476–3480.
- [11] Willauer, H. D., Collins, G. E., *Electrophoresis* 2003, *24*, 2193–2207.
- [12] Dolnik, V., Liu, S., Jovanovich, S. B., *Electrophoresis* 2000, *21*, 41–54.
- [13] Xu, H., Roddy, E. S., Roddy, T. P., Lapos, J. A., Ewing, A. G., *J. Sep. Sci.* 2004, *27*, 7–12.
- [14] Liu, S., Ren, H., Gao, Q., Roach, D. J., Loder, R. T. J., Armstrong, T. M., Mao, Q., Blaga, I., Barker, D. L., Jovanovich, S. B., *Proc. Natl. Acad. Sci. USA* 2000, *97*, 5369–5374.
- [15] Nikcevic, I., Lee, S. H., Piruska, A., Ahn, C. H., Ridgway, T. H., Limbach, P. A., Wehmeyer, K. R., Heineman, W. R., Seliskar, C. J., *J. Chromatogr. A* 2007, *1154*, 444–453.
- [16] Thorsen, T., Maerkl, S. J., Quake, S. R., *Science* 2002, *298*, 580–584.
- [17] Wu, D., Qin, J., Lin, B., *J. Chromatogr. A* 2008, *1184*, 542–559.
- [18] Cheng, S. B., Skinner, C. D., Taylor, J., Attiya, S., Lee, W. E., Picelli, G., Harrison, D. J., *Anal. Chem.* 2001, *73*, 1472–1479.
- [19] Tian, H., Emrich, C. A., Scherer, J. R., Mathies, R. A., Andersen, P. S., Larsen, L. A., Christiansen, M., *Electrophoresis* 2005, *26*, 1834–1842.
- [20] Woolley, A. T., Sensabaugh, G. F., Mathies, R. A., *Anal. Chem.* 1997, *69*, 2181–2186.
- [21] Dishinger, J. F., Kennedy, R. T., *Electrophoresis* 2008, *29*, 3296–3305.
- [22] Simpson, P. C., Roach, D., Woolley, A. T., Thorsen, T., Johnston, R., Sensabaugh, G. F., Mathies, R. A., *Proc. Natl. Acad. Sci. USA* 1998, *95*, 2256–2261.
- [23] Huang, Z., Munro, N., Huhmer, A. F. R., Landers, J. P., *Anal. Chem.* 1999, *71*, 5309–5314.
- [24] Shi, Y., Simpson, P. C., Scherer, J. R., Wexler, D., Skibola, C., Smith, M. T., Mathies, R. A., *Anal. Chem.* 1999, *71*, 5354–5361.
- [25] Paegel, B. M., Hutt, L. D., Simpson, P. C., Mathies, R. A., *Anal. Chem.* 2000, *72*, 3030–3037.
- [26] Smith, J. P., Hinson-Smith, V., *Anal. Chem.* 2001, *73*, 327A–331A.
- [27] Tan, H., Yeung, E. S., *Anal. Chem.* 1998, *70*, 4044–4053.
- [28] Wu, J., Tragas, C., Watson, A., Pawliszyn, J., *Anal. Chim. Acta* 1999, *383*, 67–78.
- [29] Smith, E. M., Xu, H., Ewing, A. G., *Electrophoresis* 2001, *22*, 363–370.
- [30] Hietpas, P. B., Bullard, K. M., Gutman, D. A., Ewing, A. G., *Anal. Chem.* 1997, *69*, 2292–2298.
- [31] Dang, F., Tabata, O., Kurokawa, M., Ewis, A. A., Zhang, L., Yamaoka, Y., Shinohara, S., Shinohara, Y., Ishikawa, M., Baba, Y., *Anal. Chem.* 2005, *77*, 2140–2146.
- [32] Dang, F., Shinohara, S., Tabata, O., Yamaoka, Y., Kurokawa, M., Shinohara, Y., Ishikawa, M., Baba, Y., *Lab Chip* 2005, *5*, 472–478.
- [33] Powell, I., *Appl. Opt.* 1987, *26*, 3705–3709.
- [34] Bewsher, A., Powell, I., Boland, W., *Appl. Opt.* 1996, *35*, 1654–1658.
- [35] Ishihama, Y., Nakamura, M., Miwa, T., Kajima, T., Asakawa, N., *J. Pharm. Sci.* 2002, *91*, 933–942.
- [36] Matoga, M., Laborde-Kummer, E., Langlois, M. H., Dallet, P., Bosc, J. J., Jarry, C., Dubost, J. P., *J. Chromatogr. A* 2003, *984*, 253–260.
- [37] Currie, C. A., Heineman, W. R., Halsall, H. B., Seliskar, C. J., Limbach, P. A., Arias, F., Wehmeyer, K. R., *J. Chromatogr. B* 2005, *824*, 201–205.
- [38] Caliaro, G. A., Herbots, C. A., *J. Pharm. Biomed. Anal.* 2001, *26*, 427–434.
- [39] Poole, S. K., Patel, S., Dehring, K., Workman, H., Poole, C. F., *J. Chromatogr. A* 2004, *1037*, 445–454.
- [40] Henchoz, Y., Schappler, J., Geiser, L., Prat, J., Carrupt, P.-A., Veuthey, J.-L., *Anal. Bioanal. Chem.* 2007, *389*, 1869–1878.
- [41] Ishihama, Y., Oda, Y., Asakawa, N., *J. Pharm. Sci.* 1994, *83*, 1500–1507.
- [42] Gong, S., Su, X., Bo, T., Zhang, X., Liu, H., Li, K. A., *J. Sep. Sci.* 2003, *26*, 549–554.
- [43] Diehl, H., Markuszewski, R., *Talanta* 1985, *32*, 159–165.
- [44] Leonhardt, H., Gordon, L., Livingston, R., *J. Phys. Chem.* 1971, *75*, 245–249.